

A simple and fast high-yield synthesis of silver nanowires

Matteo Parente^a, Max van Helvert^a, Ruben F Hamans^a, Ruth Verbroekken^a, Rochan Sinha^a, Anja Bieberle-Hutter^a, and Andrea Baldi^{a,b,‡}

^aDIFFER – Dutch Institute for Fundamental Energy Research, 5612 AJ Eindhoven, The Netherlands

^bVrije Universiteit Amsterdam, 1081 HV Amsterdam, The Netherlands

[‡]Corresponding author: a.baldi@vu.nl

Abstract

Silver nanowires (AgNWs) combine high electrical conductivity with low light absorption and scattering in the visible are therefore used in a wide range of applications, from transparent electrodes, to temperature and pressure sensors. The most common strategy for the production of AgNWs is the polyol synthesis, which always leads to the formation of silver nanoparticles as by-products. These nanoparticles degrade the performance of AgNWs based devices and have to be eliminated by several purification steps. Here, we report a simple and fast synthesis of AgNWs with minimal formation of by-products, as confirmed by the spectral purity of the final solution. Our synthetic strategy relies on the use of freshly prepared AgCl and on the minimisation of gas evolution inside the reaction vessel and drastically decreases the time and cost of AgNWs production. The observed synthetic improvements can be of general validity for the polyol synthesis of metallic nanostructures of different shapes and compositions.

Introduction

Silver nanowires (AgNWs) combine high electrical conductivity with low optical extinction in the visible, making them a cheap and flexible component of transparent conductive layers^{1–6}, strain and pressure sensors^{7–9}, temperature sensors¹⁰, substrates for surface-enhanced Raman spectroscopy¹¹, and conductive layers in photoelectrodes for solar water splitting^{12,13}. Silver nanowires are typically prepared by the so-called polyol synthesis, in which silver nitrate is dissolved in ethylene glycol (EG) in the presence of polyvinylpyrrolidone (PVP) as a stabilizing agent and a metal halide.^{2,14–17} This synthetic procedure, allows tuning of the AgNWs thickness and aspect ratio and is typically simple and cost effective. The final product, however, is always a mixture of nanowires and nanoparticles of different sizes and shapes. These by-products are detrimental for AgNWs-based applications and the as-prepared AgNWs are therefore usually subjected to several cycles of purification that increase their cost and time of production.^{2,18–20} Here we present a facile synthesis of AgNWs with a diameter of 50 nm and an average length of 10 μm with minimal formation of by-products and an extremely high optical density of the final solution.

To minimize by-products, it is important to clarify the mechanism of nanowire formation. So far, this task has been extremely challenging, as the nucleation and growth of AgNWs is reportedly influenced by a wide range

of factors, including the reaction temperature and time,²¹ the molecular weight of PVP,²² the molar ratio between AgNO₃ and PVP,²¹ the injection rate of AgNO₃,^{16,21} the concentration of halide anions,^{2,16,21,23,24} the formation of HNO₃ during the reaction,^{25,26} and even the stirring speed.²¹ In our work, we show that two often-neglected parameters for the success of the polyol synthesis are the use of freshly prepared AgCl and the minimisation of gas evolution inside the reaction vessel. The addition of silver chloride to the reaction mixture is known to lead to the growth of good quality AgNWs, although its role in the chemical process is still under debate^{2,21,27,28}. Here we report that, due to its high photosensitivity, the use of freshly prepared AgCl, as opposed to stock AgCl powder, drastically reduces the amount of by-products.

Using time-resolved analysis of the optical extinction spectra and electron microscopy images of the sample, we elucidate the shape-evolution of the AgNWs. In particular, we show that once spherical silver seed particles are formed, the growth of silver nanowires is very fast, with the reaction completing in 24 minutes at 160 °C. Moreover, after the AgNWs are formed, they can degrade back into particles, as indicated by an increase in the full width at half maximum (FWHM) of their optical extinction peak and an increase in the background extinction for $\lambda > 500$ nm. Interestingly, the nanowire degradation is faster if the reaction is let to proceed in an open container, and can be minimized by sealing the vessel and therefore suppressing bubble formation. Unlike previous reports,^{16,21} we show that in our synthesis it is possible to control the reaction kinetics by simply varying the solution temperature, without significantly changing the reaction mechanism. Such kinetic control eliminates the need for slow addition of the reactants with a syringe pump,¹⁶ making our synthesis both fast and easily scalable.

Experimental section

Chemicals

All the chemicals are used without any purification step. NaCl (>99%), AgNO₃ (>99.9999%), Polyvinylpyrrolidone (PVP, 40000 MW) and Ethylene Glycol (anhydrous, 99.8%) are purchased from Sigma Aldrich. Both Ethylene Glycol and AgNO₃ are stored in glovebox. Ultrapure water with a resistivity of 18.2 M Ω ·cm is obtained from mQ Integral Water Purification System by Merck Millipore.

Synthesis of AgCl

This synthesis is performed in the dark, due to the photosensitivity of AgCl. Silver nitrate aqueous solution (5 mL, 0.5 M) is mixed with sodium chloride aqueous solution (5 mL, 1 M) under stirring at 800 rpm for 1 minute. Upon NaCl addition, silver chloride immediately flocculates. The precipitate is separated from the supernatant, washed once with ultrapure water and dried under vacuum. The use of freshly-prepared AgCl is crucial to obtain a high yield of AgNWs as their growth depends on the availability of pentagonally twinned Ag nanoparticle nuclei.²⁷ On the contrary, the use of stock AgCl powders leads to AgNWs with a large fraction of

by-products, possibly due to the presence of partially photo-reduced AgCl providing non-optimal nucleation sites²⁹ (see also S1 and S2).

Synthesis of AgNWs

In a typical synthesis, 0.34 g of PVP (40000 MW) are dissolved into 20 mL of ethylene glycol in a 25 mL three-neck round bottom flask, and brought to 160 °C while stirring at 800 rpm. Two of the three necks of the flask are always closed with frosted glass caps soaked in a solution of ethylene glycol and PVP and wrapped with parafilm. Once the solution has reached a stable temperature, an excess (25 mg) of freshly prepared AgCl is added all at once and the solution turns from transparent to light yellow. After 3 minutes, 0.11 g of AgNO₃ are added all at once and the round bottom flask is sealed with a septum cap that is also then wrapped with parafilm.

The reaction is left under stirring at 800 rpm at 160 °C and small aliquots (<0.5 ml) are periodically taken, diluted 100 times in water, and analysed with optical spectroscopy and electron microscopy. The first aliquot is taken after 6 minutes, as no significant colour change in the solution is observed at the beginning of the reaction (see also the supplementary video). Afterwards, aliquots are taken every two minutes until the end of the reaction. The reaction mixture is left under stirring at 160 °C for 24 minutes.

Measurements

UV-Vis extinction spectra are acquired with a Perkin Elmer Lambda 1050 spectrophotometer equipped with 3D WB detector module. Scanning electron microscopy (SEM) images are acquired using a Zeiss Sigma field emission microscope operating at 5 kV.

Simulations

Numerical calculations of the extinction spectra of AgNWs are performed using 2D simulations in the Lumerical FDTD software. We simulate an infinite, pentagonally twinned silver nanowire with a circumference radius of 25 nm immersed in water and coated with a 5 nm thick PVP layer, which is typical for as-synthesized AgNWs³⁰. The corners of the pentagonal cross-section are rounded with an optimized 10 nm corner radius, to properly reproduce the spectral features observed experimentally. To approximate the optical extinction of wires randomly oriented in solution, we average over two orthogonal orientations, transverse and longitudinal with respect to the wire direction. The silver dielectric function used is from Yang³¹.

Results & discussion

Figure 1a and 1b show the evolution of the extinction spectra of the AgNWs solution during the reaction at 160 °C and 170 °C, respectively. For the synthesis at 160 °C, during the initial 6 minutes after the addition of AgNO₃,

only Ag nanoparticles^{27,32} are formed, as indicated by the symmetric plasmon resonance peak centred at around 404 nm. Between 6 and 18 minutes from the AgNO₃ addition, the spherical particles begin elongating into silver rods of growing aspect ratios, as evidenced by the broadening and red shifting of the plasmon resonance.³³ Between 18 and 24 minutes, the silver rods elongate into fully formed wires. This is indicated by the appearance of a sharp peak at 377 nm, which corresponds to the transverse resonance peak of the pentagonally-twinned AgNWs. The UV-Vis spectra of our reaction mixture provide qualitative insights on the nanowire yield of our synthesis. It is in fact well known that the width of the transverse resonance peak of AgNWs, which is influenced by the presence of irregularly shaped by-products, drastically decreases upon purification.^{20,34} Further discussion on how UV-Vis can provide insights on the yield of a silver nanowires synthesis can be found in S3.

The formation of AgNWs is accompanied by a five-fold increase of the optical density at the resonance peak from ~8 to ~40 during the transition from spheres to wires (see S4). The nanowire optical density at the end of the synthesis is comparable with the one reported for the large-scale synthesis of nanowires of similar diameters³⁴ albeit with a much narrower peak, indicating a higher yield of nanowires and a lower yield of by-products (see S5).

The slow kinetics of the transition from silver spheres to rods and the rather abrupt transition from rods to wires is highlighted for the reaction at 160 °C in Figure 1c, where we plot the time evolution of the ratio between the normalized extinction at the wires and sphere resonances, 377 nm and 404 nm, respectively. After 24 minutes of reaction at 160 °C, the silver wires slowly degrade, as indicated by the slight broadening of the transverse peak at 377 nm, which is even more evident for nanowires synthesized at 170 °C (see Figure 1d). Interestingly, the synthesis at a higher temperature leads to nanowire products with identical extinction spectra in a shorter time (see Figure 1a and 1b), as expected for thermally driven reactions.

The reaction kinetics is also dependent on the AgCl concentration, with lower amounts leading to slower nanowire growths (see section S2).

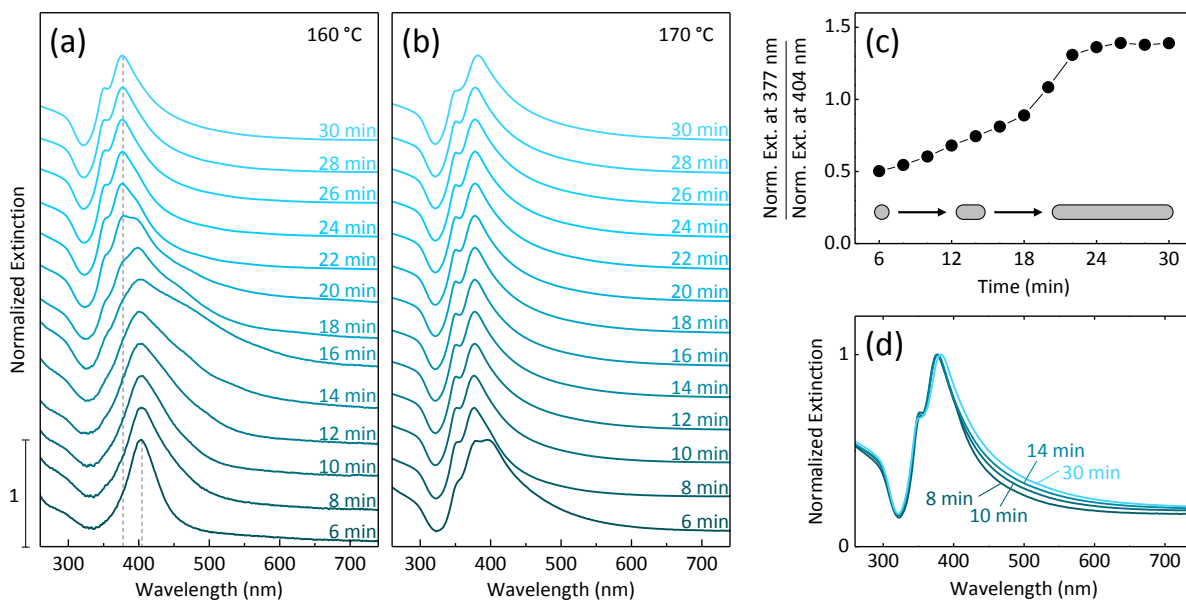


Figure 1. Time evolution of the normalized extinction spectra for the product of the AgNWs syntheses performed at (a) 160 °C and (b) 170 °C. All spectra are taken on aliquots of the as-synthesized products diluted 100 times in water and are labeled with the time elapsed from the addition of AgNO_3 . (c) Time evolution of the ratio between the normalized extinction at the AgNWs resonance ($\lambda = 377$ nm) and the initial silver nanoparticles resonance ($\lambda = 404$ nm) for the reaction carried out at 160 °C. (d) Comparison between the extinction spectra for the reaction carried out at 170 °C after 8, 10, 14, and 30 min, highlighting the AgNWs degradation and the formation of by-products.

Figure 2 shows a comparison between the extinction spectrum of our *as-synthesized* AgNWs and the one of *purified* AgNWs of similar diameters reported in the literature. The spectrum of our as-synthesized AgNWs has the narrowest peak and the lowest extinction across the visible, indicating the lowest amount of by-products. Interestingly, the only synthesis showing a spectral purity comparable to ours, albeit after one step of purification, is performed in an autoclave.³⁵ As we will later discuss, this observation further confirms the importance of suppressing gas evolution at the end of the synthesis to minimize nanowire degradation.

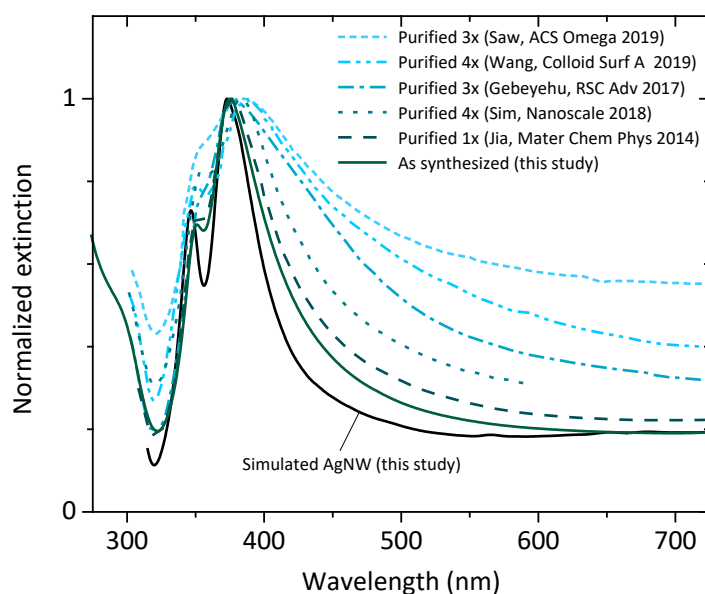


Figure 2. Normalized extinction spectra of AgNWs of similar diameters prepared by the polyol synthesis: (solid) AgNWs with a diameter of 50 nm synthesized by us at 160 °C for 24 minutes and without any purification of the final product, (dash) AgNWs with a diameter of 40 nm after one purification step for a synthesis performed in autoclave at 200 °C for 5 hours (Jia *et al.*, *Mater. Chem. Phys.* 2017, 143, 794-800)³⁵, (dot) AgNWs with a diameter of 40 nm after four purifications steps (Sim *et al.*, *Nanoscale* 2018, 10, 12087-12092)³⁶, (dash-dot) AgNWs with diameters in the range of 35-40 nm after three purification steps (Gebeyehu *et al.*, *RSC Adv.* 2017, 7, 16139-16148)¹⁷, (dash-dot-dot) AgNWs with diameter of 52 nm after four purification steps (Wang *et al.*, *Colloids Surf A* 2019, 565, 154-161)²⁸, (short dash) AgNWs with diameter of 40 nm after three purification steps (Saw *et al.*, *ACS Omega* 2019, 4, 8, 13303-13308)³⁷. The solid black line indicates the optical extinction for an ideal AgNW simulated using FDTD.

Together with the measured extinction spectra of silver nanowires from different syntheses, Figure 2 shows the simulated extinction for an ideal infinite single AgNW with a circumference radius of 25 nm immersed in water and with a PVP coating layer of 5 nm. The spectrum of our as-synthesized wires shows a FWHM and a residual extinction above 500 nm that are the closest to the ideal ones, indicating the lowest amount of by-products. Interestingly, our simulations show the existence of a physical extinction baseline of ~20% of the peak maximum for 50 nm silver nanowires above 500 nm. This residual extinction is therefore not due to the lack of purity of the synthetic product, but represents a physical extinction limit due to scattering and absorption of light by the 50 nm thick wires.

The shape evolution of the silver nanoparticles into AgNWs with a diameter of ~50 nm (see also S6) and a length of ~10 μm is confirmed by looking at representative SEM images of the synthetic products at different reaction times and temperatures, as shown in Figure 3. Similarly to the case of the extinction spectra, the SEM samples are prepared without any purification step, using the sampled aliquots diluted 100 times in water and directly drop-casted on silicon substrates.

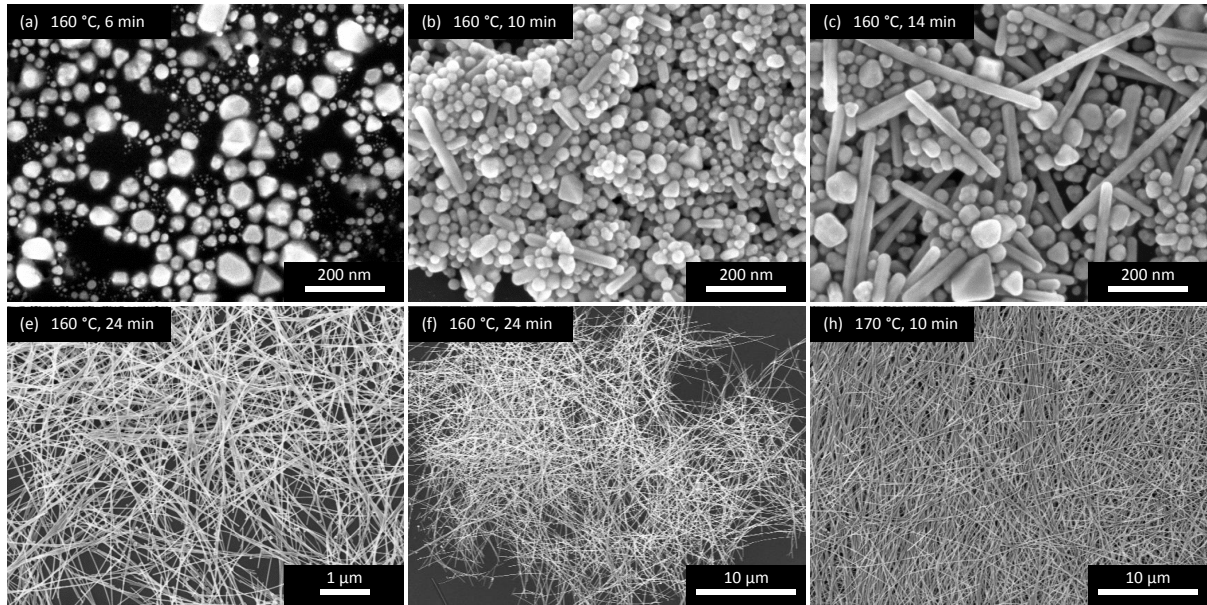
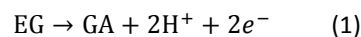
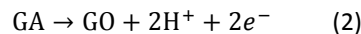


Figure 3. Scanning electron microscopy images of the products of the AgNWs synthesis after (a) 6, (b) 10, (c) 14, and (d,e) 24 min of reaction at 160 °C and (f) after 10 min of reaction at 170 °C.

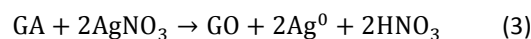
A key parameter for the successful synthesis of AgNWs and the minimization of by-product formation is the control of the reaction atmosphere. In our experiments, we show that the formation of AgNWs is followed by their slow degradation (Figure 1d). This degradation process is always accompanied by the evolution of gas bubbles at the end of the AgNWs growth (see also supplementary video) and can be understood by considering the chemical reactions involved in the nucleation and growth processes. It has been shown that the main reducing agent in the polyol synthesis, in fact, is glycoaldehyde (GA, HOCH₂CHO), which is the product of the oxidation of ethylene glycol (EG, HOCH₂CH₂OH) in the presence of oxygen at high temperatures, as indicated by Equation (1):³⁸



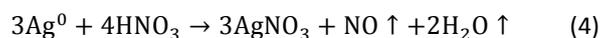
Glycoaldehyde is a strong reductant capable of reducing most noble metal ions³⁸ via its oxidation to glyoxal (GO, OCHCHO) according to Equation (2):



It is important to note that both above oxidation reactions involve the acidification of the solvent, which, in the presence of nitrate anions, can lead to the formation of nitric acid. The nucleation and growth of silver nanoparticles and nanowires must therefore be accompanied by an increased concentration of nitric acid in the ethylene glycol solvent, according to Equation (3):



At the operating temperature of 160 °C, however, the newly formed nitric acid can easily decompose into oxidizing gasses and etch the silver nanowires back into irregularly shaped Ag nanoparticles, according to Equation (4):²⁵



In a sealed reaction vessel the equilibrium constant of reaction (4) is influenced by the partial pressures of the gasses evolved upon nitric acid decomposition. According to Le Chatelier's principle, an increase in their partial pressures will shift the equilibrium toward the reactants, therefore preventing the degradation of the newly formed nanowires (see also S7). To further confirm our hypothesis that suppressing gas evolution leads to lower amount of by-products, we repeated our synthesis by varying the amount of dead volume in the reaction vessel. In agreement with the proposed mechanism above, a decrease in the dead volume, which we expect to produce an increase in the partial pressures of NO and H₂O, leads to a further decrease in nanowire degradation (see S8).

Figure 4a highlights the degradation of the AgNWs due to the development of nitric acid in solution by comparing the spectra of AgNWs suspensions after 24 and 60 minutes from the addition of AgNO₃. If the reaction is let to proceed for a total time of 60 minutes the FWHM of the AgNWs resonance peak and the extinction above 400 nm increase, indicating the degradation of the AgNWs with the formation of irregularly sized and shaped Ag nanoparticle. This interpretation is corroborated by SEM images of the sample after 60 minutes of reaction, as shown in Figure 4b, highlighting softening and bending of the AgNWs structure due to nitric acid etching. The proposed reaction mechanism is further supported by the large amount of by-products formed when carrying the reaction in a completely open flask (dotted line in Figure 4a).

Conclusions

In conclusion, we have presented a simple high throughput synthesis of silver nanowires with minimal by-products and with a straightforward relationship between the reaction time and the operating temperature. Our synthesis produces nanowires suspensions with very high optical densities and nanowire yields comparable or better than syntheses involving one or more purification steps. Furthermore, our simplified synthetic approach avoids the use of a syringe pump, drastically decreasing the production time and cost of AgNWs and making it more easily scalable toward industrial applications. The polyol synthesis is a versatile method to obtain metal nanoparticles of different shapes and compositions,³⁹⁻⁴³ used in a variety of applications, from (photo)catalysis, to batteries, colour pigments, drug delivery, and sensing^{44,45}. Nanoparticle degradation by thermal decomposition of nitric acid is a problem that affects all the polyol syntheses that involve the use of nitrate precursors, irrespective of their size or shape. Our mechanistic insights are therefore likely to extend beyond the synthesis of AgNWs.

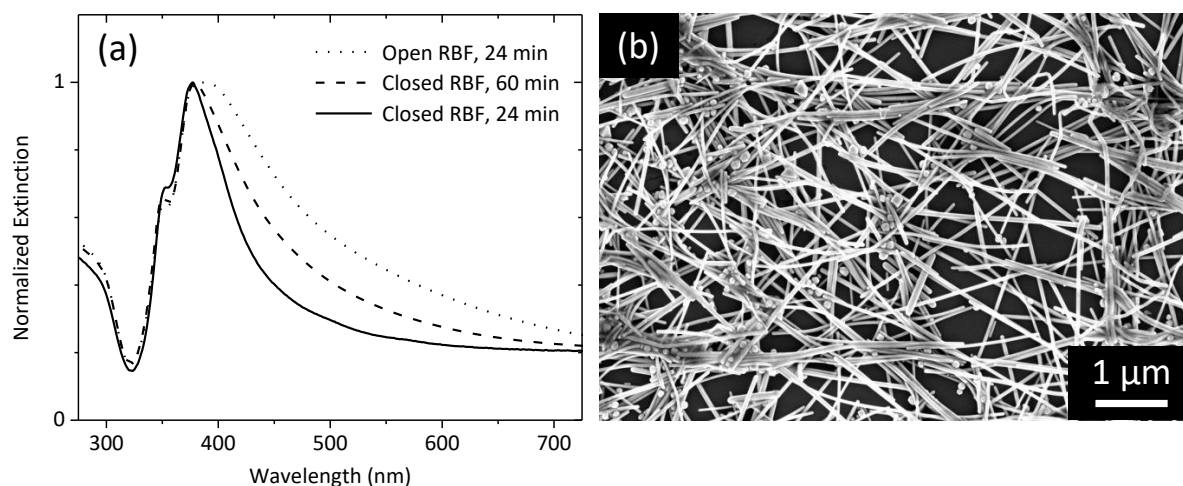


Figure 4. (a) Normalized extinction spectra for the reaction performed at 160 °C in a (solid) closed round bottom flask for 24 min, (dash) closed RBF for 60 min, and (dot) open RBF for 24 min. All spectra are taken on aliquots of the as-synthesized products diluted 100 times in water. (b) SEM picture of the AgNWs synthesized at 160 °C for 60 min, corresponding to the dashed line in panel (a).

Conflicts of interests

There are no conflicts to declare.

Acknowledgments

This work was supported by the Netherlands Organisation for Scientific Research (NWO). We gratefully acknowledge Rifat Kamarudheen, dr. Gayatri Kumari, and prof. dr. Erik Garnett for insightful discussion. We gratefully acknowledge Bram Lamers for recording and editing the supplementary video.

References

- (1) Garnett, E. C.; Cai, W.; Cha, J. J.; Mahmood, F.; Connor, S. T.; Greyson Christoforo, M.; Cui, Y.; McGehee, M. D.; Brongersma, M. L. Self-Limited Plasmonic Welding of Silver Nanowire Junctions. *Nat. Mater.* **2012**, *11* (3), 241–249.
- (2) Zhang, P.; Wyman, I.; Hu, J.; Lin, S.; Zhong, Z.; Tu, Y. Silver Nanowires : Synthesis Technologies , Growth Mechanism and Multifunctional Applications. *Mater. Sci. Eng. B* **2017**, *223*, 1–23.
- (3) Langley, D.; Bellet, D.; Simonato, J. Flexible Transparent Conductive Materials Based on Silver Nanowire Networks : A Review. *Nanotechnology* **2013**, *24*, 452001–421021.
- (4) Hu, L.; Kim, H. S.; Lee, J. Y.; Peumans, P.; Cui, Y. Scalable Coating and Properties of Transparent, Flexible, Silver Nanowire Electrodes. *ACS Nano* **2010**, *4* (5), 2955–2963.

- (5) Kang, B. M.; Xu, T.; Park, H. J.; Luo, X.; Guo, L. J. Efficiency Enhancement of Organic Solar Cells Using Transparent Plasmonic Ag Nanowire Electrodes. *Adv. Mater.* **2010**, *22*, 4378–4383.
- (6) van Hoof, N.; Parente, M.; Baldi, A.; Rivas, J. G. Terahertz Time-Domain Spectroscopy and Near-Field Microscopy of Transparent Silver Nanowire Networks. *Adv. Opt. Mater.* **2020**, *8* (3), 1–7.
- (7) Yao, S.; Zhu, Y. Wearable Multifunctional Sensors Using Printed Stretchable Conductors Made of Silver Nanowires. *Nanoscale* **2014**, *6*, 2345–2352.
- (8) Hu, W.; Niu, X.; Zhao, R.; Pei, Q. Elastomeric Transparent Capacitive Sensors Based on an Interpenetrating Composite of Silver Nanowires and Polyurethane. *Appl. Phys. Lett.* **2013**, *102* (8).
- (9) Wang, J.; Jiu, J.; Nogi, M.; Sugahara, T.; Nagao, S.; Koga, H.; He, P.; Suganuma, K. A Highly Sensitive and Flexible Pressure Sensor with Electrodes and Elastomeric Interlayer Containing Silver Nanowires. *Nanoscale* **2015**, *7* (7), 2926–2932.
- (10) Lu, Y.; Wang, M. T.; Hao, C. J.; Zhao, Z. Q.; Yao, J. Q.; Fiber, C.; With, F. Temperature Sensing Using Photonic Crystal Fiber Filled With Silver Nanowires and Liquid. *IEEE Photonics J.* **2014**, *6* (3).
- (11) Tao, A.; Kim, F.; Hess, C.; Goldberger, J.; He, R.; Sun, Y.; Xia, Y.; Yang, P. Langmuir-Blodgett Silver Nanowire Monolayers for Molecular Sensing Using Surface-Enhanced Raman Spectroscopy. *Nano Lett.* **2003**, *3* (9), 1229–1233.
- (12) Maijenburg, A. W.; Veerbeek, J.; De Putter, R.; Veldhuis, S. A.; Zoontjes, M. G. C.; Mul, G.; Montero-Moreno, J. M.; Nielsch, K.; Schäfer, H.; Steinhart, M.; et al. Electrochemical Synthesis of Coaxial TiO₂-Ag Nanowires and Their Application in Photocatalytic Water Splitting. *Journal of Materials Chemistry A*. 2014, pp 2648–2656.
- (13) I. Neelakanta Reddya, Ch. Venkata Reddya, Adem Sreedharb, Migyung Choc, Dongseob Kimd, J. S. Effect of Plasmonic Ag Nanowires on the Photocatalytic Activity of Cu Doped Fe₂O₃ Nanostructures Photoanodes for Superior Photoelectrochemical Water Splitting Applications. *J. Electroanal. Chem.* **2019**, *842*, 146–160.
- (14) Korte, K. E.; Skrabalak, S. E.; Xia, Y. Rapid Synthesis of Silver Nanowires through a CuCl- or CuCl₂-Mediated Polyol Process. *J. Mater. Chem.* **2008**, *18* (4), 437–441.
- (15) Liu, Y.; Chen, Y.; Shi, R.; Cao, L.; Wang, Z.; Sun, T.; Lin, J.; Liu, J.; Huang, W. High-Yield and Rapid Synthesis of Ultrathin Silver Nanowires for Low-Haze Transparent Conductors. *RSC Adv.* **2017**, *7* (9), 4891–4895.
- (16) Da Silva, R. R.; Yang, M.; Choi, S. Il; Chi, M.; Luo, M.; Zhang, C.; Li, Z. Y.; Camargo, P. H. C.; Ribeiro, S. J. L.; Xia, Y. Facile Synthesis of Sub-20 Nm Silver Nanowires through a Bromide-Mediated Polyol Method. *ACS Nano* **2016**, *10* (8), 7892–7900.
- (17) Gebeyehu, M. B.; Chala, T. F.; Chang, S. Y.; Wu, C. M.; Lee, J. Y. Synthesis and Highly Effective

- Purification of Silver Nanowires to Enhance Transmittance at Low Sheet Resistance with Simple Polyol and Scalable Selective Precipitation Method. *RSC Adv.* **2017**, *7* (26), 16139–16148.
- (18) Mayousse, C.; Celle, C.; Moreau, E.; Mainguet, J. F.; Carella, A.; Simonato, J. P. Improvements in Purification of Silver Nanowires by Decantation and Fabrication of Flexible Transparent Electrodes. Application to Capacitive Touch Sensors. *Nanotechnology* **2013**, *24* (21), 1–6.
- (19) Li, B.; Ye, S.; Stewart, I. E.; Alvarez, S.; Wiley, B. J. Synthesis and Purification of Silver Nanowires to Make Conducting Films with a Transmittance of 99%. *Nano Lett.* **2015**, *15* (10), 6722–6726.
- (20) Wan, M.; Tao, J.; Jia, D.; Chu, X.; Li, S.; Ji, S.; Ye, C. High-Purity Very Thin Silver Nanowires Obtained by Ostwald Ripening-Driven Coarsening and Sedimentation of Nanoparticles. *CrystEngComm* **2018**, *20* (20), 2834–2840.
- (21) Coskun, S.; Aksoy, B.; Unalan, H. E. Polyol Synthesis of Silver Nanowires: An Extensive Parametric Study. *Cryst. Growth Des.* **2011**, *11* (11), 4963–4969.
- (22) Zeng, X.; Zhou, B.; Gao, Y.; Wang, C.; Li, S.; Yeung, C. Y.; Wen, W. J. Structural Dependence of Silver Nanowires on Polyvinyl Pyrrolidone (PVP) Chain Length. *Nanotechnology* **2014**, *25* (49).
- (23) Schuette, W. M.; Buhro, W. E. Silver Chloride as a Heterogeneous Nucleant for the Growth of Silver Nanowires. *ACS Nano* **2013**, *7* (5), 3844–3853.
- (24) An, C.; Wang, J.; Wang, S.; Zhang, Q.; Yang, M.; Zhan, J. Converting AgCl Nanocubes to Silver Nanowires through a Glycerol-Mediated Solution Route. *CrystEngComm* **2012**, *14* (18), 5886–5891.
- (25) Whitcomb, D. R.; Clapp, A. R.; Bühlmann, P.; Blinn, J. C.; Zhang, J. New Perspectives on Silver Nanowire Formation from Dynamic Silver Ion Concentration Monitoring and Nitric Oxide Production in the Polyol Process. *Cryst. Growth Des.* **2016**, *16* (4), 1861–1868.
- (26) Zhang, W.; Chen, P.; Gao, Q.; Zhang, Y.; Tang, Y. High-Concentration Preparation of Silver Nanowires: Restraining in Situ Nitric Acidic Etching by Steel-Assisted Polyol Method. *Chem. Mater.* **2008**, *20* (5), 1699–1704.
- (27) Zhang, S.; Jiang, Z.; Xie, Z.; Xu, X.; Huang, R. Growth of Silver Nanowires from Solutions : A Cyclic Penta-Twinned-Crystal Growth Mechanism. *J. Phys. Chem. B* **2005**, *109*, 9416–9421.
- (28) Wang, H.; Wang, Y.; Chen, X. Synthesis of Uniform Silver Nanowires from AgCl Seeds for Transparent Conductive Films via Spin-Coating at Variable Spin-Speed. *Colloids Surfaces A Physicochem. Eng. Asp.* **2019**, *565* (August 2018), 154–161.
- (29) Shinsaku Fujita. *Organic Chemistry of Photography*; Springer, Berlin, H., Ed.; 2004.
- (30) Hwang, J.; Shim, Y.; Yoon, S. M.; Lee, S. H.; Park, S. H. Influence of Polyvinylpyrrolidone (PVP) Capping Layer on Silver Nanowire Networks: Theoretical and Experimental Studies. *RSC Adv.* **2016**, *6* (37),

30972–30977.

- (31) Yang, H. U.; D'Archangel, J.; Sundheimer, M. L.; Tucker, E.; Boreman, G. D.; Raschke, M. B. Optical Dielectric Function of Silver. *Phys. Rev. B - Condens. Matter Mater. Phys.* **2015**, *91* (23), 1–11.
- (32) Sun, Y.; Mayers, B.; Herricks, T.; Xia, Y. Polyol Synthesis of Uniform Silver Nanowires: A Plausible Growth Mechanism and the Supporting Evidence. *Nano Lett.* **2003**, *3* (7), 955–960.
- (33) Lee, K. S.; El-Sayed, M. A. Gold and Silver Nanoparticles in Sensing and Imaging: Sensitivity of Plasmon Response to Size, Shape, and Metal Composition. *J. Phys. Chem. B* **2006**, *110* (39), 19220–19225.
- (34) Sun, Y.; Yin, Y.; Mayers, B. T.; Herricks, T.; Xia, Y. Uniform Silver Nanowires Synthesis by Reducing AgNO₃ with Ethylene Glycol in the Presence of Seeds and Poly(Vinyl Pyrrolidone). *Chem. Mater.* **2002**, *14* (11), 4736–4745.
- (35) Jia, C.; Yang, P.; Zhang, A. Glycerol and Ethylene Glycol Co-Mediated Synthesis of Uniform Multiple Crystalline Silver Nanowires. *Mater. Chem. Phys.* **2014**, *143* (2), 794–800.
- (36) Sim, H.; Kim, C.; Bok, S.; Kim, M. K.; Oh, H.; Lim, G. H.; Cho, S. M.; Lim, B. Five-Minute Synthesis of Silver Nanowires and Their Roll-to-Roll Processing for Large-Area Organic Light Emitting Diodes. *Nanoscale* **2018**, *10* (25), 12087–12092.
- (37) Saw, M. J.; Ghosh, B.; Nguyen, M. T.; Jirasattayaporn, K.; Kheawhom, S.; Shirahata, N.; Yonezawa, T. High Aspect Ratio and Post-Processing Free Silver Nanowires as Top Electrodes for Inverted-Structured Photodiodes. *ACS Omega* **2019**, *4* (8), 13303–13308.
- (38) Skrabalak, S. E.; Wiley, B. J.; Kim, M.; Formo, E. V.; Xia, Y.; V, W. U.; Louis, S. On the Polyol Synthesis of Silver Nanostructures : Glycolaldehyde as a Reducing Agent. *Nano Lett.* **2008**, *8*, 1–5.
- (39) Herricks, T.; Chen, J.; Xia, Y. Polyol Synthesis of Platinum Nanoparticles: Control of Morphology with Sodium Nitrate. *Nano Lett.* **2004**, *4* (12), 2367–2371.
- (40) Wiley, B.; Sun, Y.; Mayers, B.; Xia, Y. Shape-Controlled Synthesis of Metal Nanostructures: The Case of Silver. *Chem. - A Eur. J.* **2005**, *11* (2), 454–463.
- (41) Wiley, B.; Sun, Y.; Xia, Y. Polyol Synthesis of Silver Nanostructures: Control of Product Morphology with Fe(II) or Fe(III) Species. *Langmuir* **2005**, *21* (18), 8077–8080.
- (42) Skrabalak, S. E.; Au, L.; Li, X.; Xia, Y. Facile Synthesis of Ag Nanocubes and Au Nanocages. *Nat. Protoc.* **2007**, *2* (9), 2182–2190.
- (43) Xiong, Y.; Siekkinen, A. R.; Wang, J.; Yin, Y.; Kim, M. J.; Xia, Y. Synthesis of Silver Nanoplates at High Yields by Slowing down the Polyol Reduction of Silver Nitrate with Polyacrylamide. *J. Mater. Chem.* **2007**, *17* (25), 2600–2602.
- (44) Dong, H.; Chen, Y. C.; Feldmann, C. Polyol Synthesis of Nanoparticles: Status and Options Regarding

Metals, Oxides, Chalcogenides, and Non-Metal Elements. *Green Chem.* **2015**, *17* (8), 4107–4132.

- (45) Fievet, F.; Ammar-Merah, S.; Brayner, R.; Chau, F.; Giraud, M.; Mammeri, F.; Peron, J.; Piquemal, J. Y.; Sicard, L.; Viau, G. The Polyol Process: A Unique Method for Easy Access to Metal Nanoparticles with Tailored Sizes, Shapes and Compositions. *Chem. Soc. Rev.* **2018**, *47* (14), 5187–5233.